TEXTON-BASED SEGMENTATION AND CLASSIFICATION OF HUMAN EMBRYONIC STEM CELL COLONIES USING MULTI-STAGE BAYESIAN LEVEL SETS

Nathan Lowry[1,2]*, Rami Mangoubi*[1]*, Mukund Desai*[1]*, Youssef Marzouk*[2]*, and Paul Sammak*[3]

[1]C.S. Draper Laboratory, Cambridge, MA, 02139
[2]Massachusetts Institute of Technology, Cambridge, MA, 02139
[3]University of Pittsburgh, Pittsburgh, PA 15213

ABSTRACT

We present a texton-based, multi-stage Bayesian level set algorithm which we use to segment colony images of hESC and their derivatives. We extend our previous research segmenting stem cells according to multiresolution texture methods to accommodate colonies and tissues with diffuse and varied textures via a filter bank approach similar to the MR8. Texture features computed for test images are classified via comparison with learned sets of class-specific textural primitives, known as textons. Encompassing this texture model is the new Bayesian level set algorithm, which smoothes and regularizes classification similar to level sets but is simpler in its probabilistic implementation. The resulting algorithm accurately and automatically classifies images of pluripotent hESC and trophectoderm colonies for high-content screening applications.

Index Terms: Bayesian level set, classification, segmentation, stem cell, MR8, texture analysis.

1. INTRODUCTION

Pluripotent human embryonic stem cells (hESC) and their derivatives present exciting research opportunities but must be continually monitored to prevent unsupervised differentiation and insure successful fate control. Visual inspection offers a non-invasive alternative to destructive chemical testing, but sufficiently trained microscopists have limited time, are expensive to train, and may yield subjective results, acute shortcomings in high-throughput screening applications.

We have previously [4] used multiresolution wavelet texture analysis to automate the visual classification of stem cells in homogenous textural patches have been manually selected by a researcher. In [3], we developed the *Bayesian level set* (BLS) algorithm, which combines many of the advantages of level set segmentation (noise suppression, smoothing and regularization of class borders) with the ease of implementation of the common finite mixture model expectation-maximization algorithm and showed that it could be used to automatically segment induced pluripotent stem cell colonies from their background growth media according to wavelet features.

Despite enabling successful classification, wavelet texture methods prove unsuitable for segmenting certain cell colony images, including trophectoderm (TE), a hESC derivative. Unlike the tight, textured hESCs, TE exhibits large, dark cells in a diffuse matrix and is better modeled by blob or bar detectors at particular scales rather than wavelet high-pass subbands.

To segment these colony images, we build upon our work in [3] by incorporating texton-based methods [2, 6, 7] into the BLS. Textons, which model texture according to a learned dictionary of feature vectors, require a multi-stage BLS that hierarchically proceeds from class (pluripotent, TE, growth media) through a library of textons to the image features. This novel approach automates the segmentation of pluripotent hESC and TE images, towards the long term goal of automatic stem cell cultivation and assessment of experiments.

2. TEXTURE-BASED BAYESIAN LEVEL SETS

2.1. Texton-Based Texture Classification

Recent texture classification efforts model texture via a set of primitives (i.e. textons) which define what a texture locally "looks like." Several methods exist for calculating these textons, including statistical modeling of image patch exemplars [6] and compressive sensing techniques [2], but we adopt the MR8 approach of [7], which models texture by convolving the image with a filter bank containing Gaussian (local mean) and Laplacian-of-Gaussian (LoG, blob detector) filters at fixed scale and edge and bar filters at three different scales and several orientations. The texton is the vector of eight filter responses at a given pixel.

To classify an image texture patch, a texton dictionary must first be learned for each class; we denote as $\mu_{t|c}$ the t^{th} learned feature vector for class c. Texturally homogeneous images may be classified by comparing the statistics of image textons to these learned dictionaries [7]. We segment texturally inhomogeneous images according to the multi-stage Bayesian level set algorithm described below.

Work supported by NIH grant 1 R01 EB006161-01A4 and by an internal research and development grant from the C.S. Draper Laboratory, Cambridge, MA.

2.2. Bayesian Level Sets

In [3], we introduced the Bayesian level set algorithm to solve the level set problem in a manner similar to the finite mixture model Expectation-Maximization algorithm. Like level sets, the BLS rejects noise and produces segmentations with smooth, regular borders, but it is simpler in implementation, requiring no solution of PDEs or maintenance of the level set surface ϕ and is much more tolerant of poor initial conditions. Furthermore, the BLS may be easily extended to an arbitrary number of classes without requiring additional computational machinery to eliminate overlap between regions or fill gaps as in many multiphase level set algorithms.

Level set region competition [8] segments an image into classes c_0 and c_1 by minimizing a functional of surface ϕ:

$$\begin{aligned} E(\phi, \Theta; Y) = \lambda \int_\Omega \|\nabla H(\phi(x))\| \mathrm{d}x \\ - \int_\Omega H(\phi(x)) \cdot \log p(Y(x) \mid Z(x) = c_0; \Theta)\, \mathrm{d}x \\ - \int_\Omega H(-\phi(x)) \cdot \log p(Y(x) \mid Z(x) = c_1; \Theta)\, \mathrm{d}x \end{aligned} \tag{1}$$

$Z(x)$ is the true classification and assigns each pixel x in the image domain Ω a label from set $\mathcal{C}$. Observations $Y(x)$ are generated stochastically from $Z(x)$ according to parameters Θ. The regularized Heaviside step function $H(\cdot)$ demarcates the two regions ($c_0 = \{x \mid \phi(x) > 0\}$), so the *zero level set* of ϕ partitions the image. Constant λ penalizes the length of the segmenting contour. The minimizing condition is:

$$0 = \log \frac{p(Y(x) \mid Z(x) = c_0; \Theta)}{p(Y(x) \mid Z(x) = c_1; \Theta)} + \lambda \kappa(\phi(x)) \qquad \forall x \in \Omega \tag{2}$$

where $\kappa(\phi)$ is the curvature of the iso-contours of ϕ.

By applying the "log-odds" approach of [5]:

$$\phi(x) = \log \frac{p(Z(x) = c_0 \mid Y(x); \Theta)}{p(Z(x) = c_1 \mid Y(x); \Theta)} \tag{3}$$

we derive a Bayesian procedure for solving for (2). We present the results below, referring the reader to [3] for the derivation.

At each iteration k, the *Bayesian Level Set* (BLS) algorithm refines image classification in two steps. *First*, update soft classification $p(Z \mid Y; \Theta)$ via Bayes' rule. *Second*, estimate parameters Θ via maximum likelihood.

The second sub-iteration is self-explanatory, and we focus on the first. For compactness, we abbreviate as $q^k_{Z|Y}(c)$ the probability at iteration k that pixel x is a member of class $c \in \mathcal{C}$ conditioned on data $Y(x)$ and parameters Θ estimated at the previous iteration, i.e. $p_k(Z(x) = c \mid Y(x); \Theta_{k-1})$. Likewise, prior and conditional probabilities $p_k(Z(x) = c)$ and $p_k(Y(x) \mid Z(x) = c; \Theta_{k-1})$ are $q^k_Z(c)$ and $q^k_{Y|Z}(c)$. Update according to Bayes' rule:

$$q^k_{Z|Y}(c) = \frac{q^k_{Y|Z}(c)\, q^k_Z(c)}{\sum_{l \in \mathcal{C}} q^k_{Y|Z}(l)\, q^k_Z(l)} \tag{4}$$

The *smoothing prior* q^{k+1}_Z is calculated from the previous log-likelihood of classification, smoothed via flow-by-curvature:

$$\begin{aligned} q^k_Z(c) &= \left(1 + e^{-L^{k-1}(c)}\right)^{-1} \\ L^{k-1}(c) &= \log \frac{q^{k-1}_{Z|Y}(c)}{1 - q^{k-1}_{Z|Y}(c)} + \lambda \kappa\left(q^{k-1}_{Z|Y}(c)\right) \end{aligned} \tag{5}$$

Multi-region smoothing priors are then normalized to one.

With this smoothing prior, (4) reaches steady state at the minimizing condition in (2). Such a prior effectively creates stochastic dependence in a localized neighborhood in order to encourage local classification similarity and is analogous to atlas-based EM classification. In the absence of a pre-defined probabilistic classification atlas, we iteratively estimate one by smoothing the previous soft classification. In certain applications, it may be desirable to substitute other smoothing functions for flow-by-curvature, e.g. Gaussian diffusion.

2.3. Multi-stage Bayesian Level Sets

The BLS implicitly assumes that observations Y are generated via a two-stage Markov process: First, a class is selected for each pixel according to some prior function q_Z, after which observations are generated from parameters Θ.

We accommodate texton-based classification by adding an intermediate stage to the BLS. After determining class Z via prior (5), a texton T is selected from a set of primitives $\mathcal{T}_Z$ specific to class Z according to a second prior $p(T \mid Z; \Theta)$, denoted $q_{T|Z}$. Lastly, generate Y from T via $p(Y \mid T; \Theta)$, denoted $q_{Y|T}$, which is conditionally independent of Z. The intuition is that class is locally similar, but textons within a class may be arbitrarily jumbled; the prior in (5) thus encourages smoothness in Z, while the prior in (7) allows for freedom in spatially assigning textons T within class Z.

At iteration k, sub-iteration 1, we determine $q^k_{Z|Y}(c)$ by marginalizing with respect to $\mathcal{T}_c$:

$$q^{k+1}_{Z|Y}(c) = \frac{q^{k+1}_Z(c) \sum_{t \in \mathcal{T}_c} q^{k+1}_{T|Z}(t, c)\, q^{k+1}_{Y|T}(t)}{\sum_{l \in \mathcal{C}} q^{k+1}_Z(l) \sum_{s \in \mathcal{T}_l} q^{k+1}_{T|Z}(s, l)\, q^{k+1}_{Y|T}(s)} \tag{6}$$

$q^k_{T|Z}(t, c)$ is a constant $\pi^k_{t|c}$, and $q^k_{Y|T}(t)$ is normal about $\mu_{t|c}$ with covariance $\Sigma^k_{t|c}$:

$$q^{k+1}_{T|Z}(t, c) = \pi^k_{t|c} \tag{7}$$

$$q^{k+1}_{Y|T}(t) \sim N\left(Y; \mu_{t|c}, \Sigma^k_{t|c}\right) \tag{8}$$

In sub-iteration 2, we estimate parameters:

$$\pi^{k+1}_{t|c} = \frac{1}{N(c)} \sum_\Omega q^{k+1}_{Z|Y}(c)\, q^{k+1}_{T|Y,Z}(t, c) \tag{9}$$

$$\Sigma^{k+1}_{t|c} = \frac{1}{N(c)} \sum_\Omega \left[\begin{array}{l} q^{k+1}_{Z|Y}(c)\, q^{k+1}_{T|Y,Z}(t, c) \\ \cdot \left(Y - \mu_{t|c}\right) \left(Y - \mu_{t|c}\right)^T \end{array} \right] \tag{10}$$

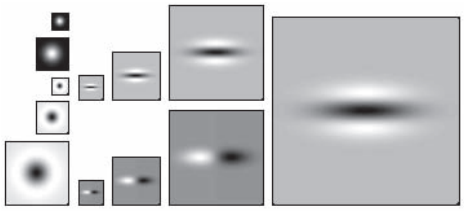


Fig. 1. *Texture Filters* used for texton generation.

$$N(c) = \sum_{\Omega} q^{k+1}_{Z|Y}(c) \sum_{s \in \mathcal{T}_c} q^{k+1}_{T|Y,Z}(s,c) \tag{11}$$

$$q^{k+1}_{T|Y,Z}(t,c) = \frac{q^{k+1}_{Y|T}(t)\, q^{k+1}_{T|Z}(t,c)}{\sum_{s \in \mathcal{T}_c} q^{k+1}_{Y|T}(s)\, q^{k+1}_{T|Z}(s,c)} \tag{12}$$

$\mu_{t|c}$ are constant textons learned *a priori* (cf. subsection 2.1), and Y are responses from filters selected in subsection 3.2.

3. APPLICATION TO STEM CELL COLONIES

3.1. Data Collection

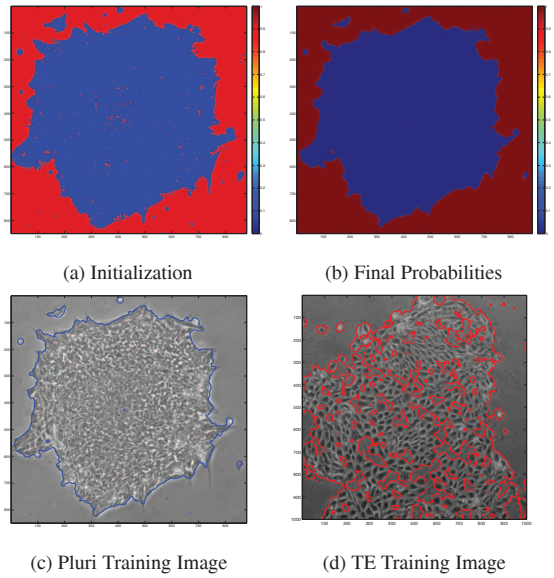
Pluripotent hESCs, line H7, were grown feeder-free on Geltrex-coated plates (Invitrogen) and maintained in StemPro (Invitrogen), a defined pluripotency media. Media was changed every other day and colonies were passaged weekly with Collagenase Type IV. Specific and selective differentiation to an epithelial cell type was achieved by culturing for four days in EMIM basal media without bFGF but with the addition of BMP-4 (100ng/mL) to the media [1].

Colonies were imaged via phase-contrast microscopy using a 4x Nikon 0.13 NA objective on a TMS cell culture microscope with a 10M Pixel Nikon D40x SLR camera. Images were reduced to grayscale from the green channel to reduce chromatic aberration and avoid color registration errors.

3.2. Texture Feature Selection and Training

The eight MR8 features were scaled to a particular database [7], so we applied a variety of features to the manually classified images in figure 2c-d to select the scales relevant to our data. The twelve most relevant features were selected according to mutual information (MI): Gaussian at $\sigma = \{2, 4\}$, LoG at $\sigma = \{2, 4, 8\}$, bar filters at $\sigma = \{1, 2, 4, 8\}$, and edge filters at $\sigma = \{1, 2, 4\}$. Selected filters are shown in figure 1.

A texton library was then learned from these images using a greedy search: First, assign each texton in a particular class to an active list. Then score each texton i in the list according to size of set S_i, the textons in that class closer to i than to any texton in another class. Add the texton j with the highest score to the library, and remove j and S_j from the active list. Repeat, re-scoring and adding textons to the library.



(a) Initialization (b) Final Probabilities

(c) Pluri Training Image (d) TE Training Image

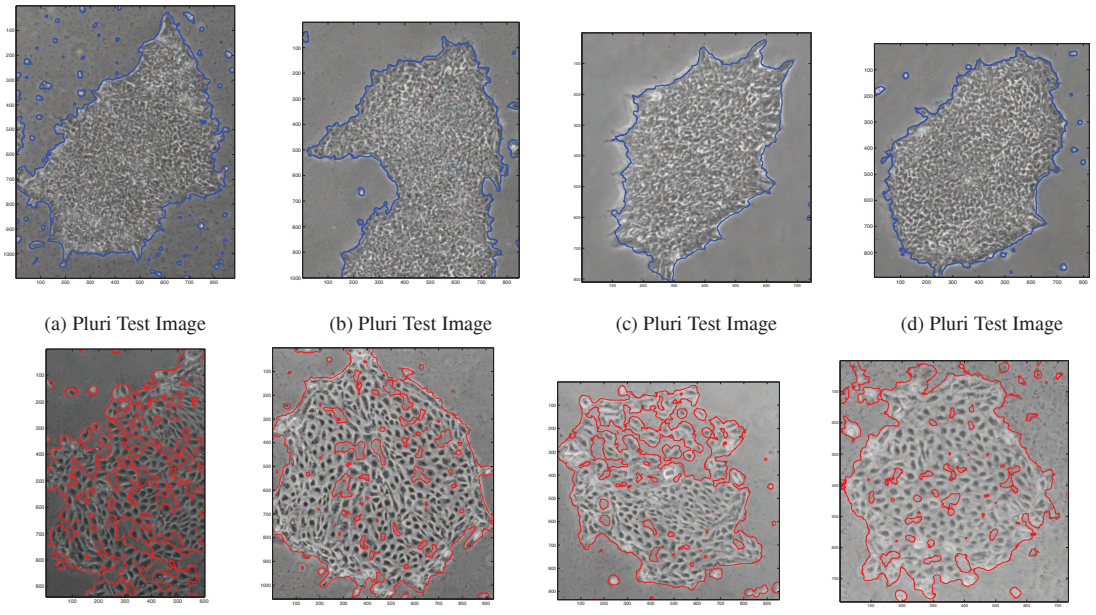
Fig. 2. *Training and Segmentation Process for Stem Cell Segmentation* (a) Regions are initialized according to the closest texton, note the way the initial labeling bleeds out into the phase halo; (b) Final probability map, which has eliminated most of the phase halo; (c) Pluripotent training image, threshold (b) to obtain the contour; (d) Trophectoderm training image, note that the algorithm correctly classifies holes interior to the colony as growth media.

3.3. Results and Analysis

Figure 2 illustrates the training and segmentation process for the texton-based, multi-stage BLS applied to pluripotent hESC and TE cell colonies. In figure 2a, initial conditions were automatically determined by finding the texton with the minimum Euclidean distance to a particular pixel and setting the corresponding class probability to 0.9. Final class probabilities, as determined by the BLS, are shown in figure 2b, and contours in figure 2c indicate where $q_{Z|Y} = 0.5$. Regions interior to the contour are classified as cell colony and exterior regions as growth media.

Figure 2c is a proof-of-concept where the BLS correctly segments the image used to train the pluripotent texton library with a tight border excluding most of the phase halo. This imaging artifact appears as a white band around the colony and has a significant filter response. Thresholding in the texture space would assign it to the colony, so the texture library is trained to recognize it. False positives consist of dead cells (white blips at the top and top left) and extracellular protein (black streak at right). With similar scale and appearance to the colony, these are difficult to distinguish texturally. As shown in figures 3a-d, the BLS exhibits similar performance when applied to test images not used to train the library.

Figure 2d is another proof-of-concept where the BLS correctly segments the image used to train the TE library. TE



(a) Pluri Test Image (b) Pluri Test Image (c) Pluri Test Image (d) Pluri Test Image

(e) TE Test Image (f) TE Test Image (g) TE Test Image (h) TE Test Image

Fig. 3. *Texture-Based Multi-stage BLS Segmentation of Stem Cell Colonies* (a)-(d) Pluripotent test images, note dead cells and extracellular proteins (dark streaks) in (a) classified as pluripotent; (e)-(h) TE test images, note the correct classification of extracellular proteins. Note that scale is marked for each figure and is not uniform.

is fairly diffuse, yet the BLS successfully finds internal holes too tedious for manual delineation. Figures 3e-h demonstrate that the BLS exhibits similar performance when applied to test TE images not used to train the library. Figure 3h is particularly interesting; despite the visual difference between the colony and the growth media in the upper right, their wavelet subband coefficients are statistically similar, making these regions difficult to distinguish using multiresolution methods. Save for a few misclassified regions, the texton-based, multi-stage BLS accurately locates the colony border.

4. CONCLUSION

Multi-stage Bayesian level sets allow for texture-based segmentation using learned texton dictionaries. Though our current approach uses filter bank methods, this scheme is easily extensible to texton models such as patch exemplars or compressive sensing. Like level sets, the BLS encompassing the texture model encourages smoothness in the segmentation to regularize classification and suppress noise but is simpler in implementation. Results shown indicate present ability to successfully and automatically segment pluripotent hESC and trophectoderm colonies despite the presence of distracting external objects, including dead cells and extracellular protein. In the future, we intend to extend the texton library to additional colony and tissue types.

5. REFERENCES

[1] T.M. Erb, C. Scheider, S.E. Mucko, J.S. Sanfilippo, N.C. Lowry, M.N. Desai, R.S. Mangoubi, S.H. Leuba, and P.J. Sammak. "Paracrine and epigenetic control of trophectoderm differentiation from human embryonic stem cells: etc." *Stem Cells Dev.* 20.9 (September 2011) 1601-1614.

[2] L. Liu and P. Fiegurth. "Texture Classification Using Compressed Sensing." *Canadian Conf. Comp. and Robot Vis.* 2010.

[3] N. Lowry, R. Mangoubi, M. Desai, Y. Marzouk, and P. Sammak. "A Unified Approach to Expectation-Maximization and Level Set Segmentation Applied to Stem Cell and Brain MRI Images." *ISBI* 2011.

[4] R. Mangoubi, C. Jeffreys, A. Copeland, M. Desai, and P. Sammak. "Non-Invasive Image Based Support Vector Machine Classification of Human Embryonic Stem Cells." *ISBI* 2007.

[5] K. Pohl, R. Kikinis, and W. Wells. "Active Mean Fields: Solving the Mean Field Approximation in the Level Set Framework." *IPMI* 2007, *LNCS* 4584 (2007) 26-37.

[6] M. Varma and A. Zisserman. "A Statistical Approach to Material Classification Using Image Patch Exemplars." *IEEE Trans. PAMI* 31.11 (Nov. 2009) 2032-2047.

[7] M. Varma and A. Zisserman. "A Statistical Approach to Texture Classification from Single Images." *Int'l J. Computer Vision* 62.1/2 (2005) 61-81.

[8] S. Zhu and A. Yuille. "Region Competition: Unifying Snakes, Region Growing, and Bayes/MDL for Multiband Image Segmentation." *IEEE Trans. PAMI* 18.9 (Sept. 1996) 884-900.